AGU PUBLICATIONS

Geophysical Research Letters

RESEARCH LETTER
10.1002/2016GL070460

Key Points:
- Previous studies have analyzed winter warming by averaging the first two postvolcanic winters and have included smaller eruptions
- CMIP5 models show an ability to produce winter warming in the first year after tropical volcanic eruptions
- The CMIP5 historical ensemble shows a clear reduction of summer monsoon rainfall

Supporting Information:
- Supporting Information S1

Correspondence to:
B. Zambri,
bzambri@envsci.rutgers.edu

Citation:
Zambri, B., and A. Robock (2016), Winter warming and summer monsoon reduction after volcanic eruptions in Coupled Model Intercomparison Project 5 (CMIP5) simulations, *Geophys. Res. Lett.*, *43*, 10,920–10,928, doi:10.1002/2016GL070460.

Received 14 JUL 2016
Accepted 4 OCT 2016
Accepted article online 6 OCT 2016
Published online 22 OCT 2016

Winter warming and summer monsoon reduction after volcanic eruptions in Coupled Model Intercomparison Project 5 (CMIP5) simulations

Brian Zambri[1] and Alan Robock[1]

[1]Department of Environmental Sciences, Rutgers University, New Brunswick, New Jersey, USA

Abstract Though previous studies have shown that state-of-the-art climate models are rather imperfect in their simulations of the climate response to large volcanic eruptions, the results depend on how the analyses were done. Observations show that all recent large tropical eruptions were followed by winter warming in the first Northern Hemisphere (NH) winter after the eruption, with little such response in the second winter, yet a number of the evaluations have combined the first and second winters. We have looked at just the first winter after large eruptions since 1850 in the Coupled Model Intercomparison Project 5 historical simulations and find that most models do produce a winter warming signal, with warmer temperatures over NH continents and a stronger polar vortex in the lower stratosphere. We also examined NH summer precipitation responses in the first year after these large volcanic eruptions and find clear reductions of summer monsoon rainfall.

1. Introduction

Large volcanic eruptions inject sulfur gases into the stratosphere. Over a period of weeks, the sulfur gas is converted to sulfate aerosols [*Robock*, 2000]. Sulfate aerosols decrease direct radiation and increase diffuse radiation as it scatters incoming shortwave radiation, with a net decrease in incoming shortwave radiation resulting in a cooling of Earth's surface [*Robock and Mao*, 1995; *Robock*, 2000]. Sulfate aerosols injected into the tropical stratosphere are transported poleward with a global *e*-folding lifetime of about 1 year, meaning climate impacts of large volcanic eruptions can last up to several years [*Robock and Mao*, 1995].

On the other hand, sulfate aerosols also absorb incoming near-infrared and outgoing longwave radiation. For tropical volcanic eruptions, this absorption causes local heating in the equatorial lower stratosphere, creating greater-than-normal temperature and density gradients between the equator and poles. These anomalous gradients result in a strengthened stratospheric polar vortex, with strengthened zonal winds leading to positive temperature anomalies over northern Eurasia and sometimes parts of North America, along with significant cooling in the Middle East [*Robock and Mao*, 1992; *Perlwitz and Graf*, 1995; *Robock*, 2000].

Perlwitz and Graf [1995] and *Kodera et al*. [1996], among others, have associated a strong polar vortex with a positive phase of the North Atlantic Oscillation (NAO)—an index of the wintertime variability of north-south Northern Hemisphere (NH) sea level pressure gradients between 110°W and 70°E [*Hurrell*, 1995; *Christiansen*, 2008]—or the Arctic Oscillation (AO), the first empirical orthogonal function of NH winter monthly sea level pressure anomalies [*Thompson and Wallace*, 1998]. A positive AO corresponds to anomalously low pressure over the pole, and anomalously high pressure at midlatitudes, with the anomalies changing signs in the negative phase. After large volcanic eruptions a positive phase of the AO has been observed for the following one to two winters [*Robock and Mao*, 1992; *Stenchikov et al*., 2002].

Previous studies have concluded that climate model simulations of the historical period have largely failed at reproducing this dynamical response, having only been able to produce a slightly strengthened stratospheric vortex, and failing to reproduce a positive AO and warming/cooling patterns over Eurasia and the Middle East respectively for the two NH winters following volcanic eruptions [*Stenchikov et al*., 2006; *Driscoll et al*., 2012; *Charlton-Perez et al*., 2013]. *Driscoll et al*. [2012] analyzed historical runs from 13 models conducted for the Coupled Model Intercomparison Project 5 (CMIP5) [*Taylor et al*., 2012]. Their requirements for inclusion of a model were that the model must have at least two ensemble members and that the model must be forced with volcanic aerosols in the stratosphere. That is, *Driscoll et al*. [2012] excluded those models that either did not represent volcanic aerosols or represented them by a reduction in the solar constant. They found that consistent with the results of *Stenchikov et al*. [2006], the increase in geopotential height in the lower

stratosphere at low latitudes was reproduced by all the models. On the other hand, they found that the models showed less agreement with the negative anomalies in the polar lower stratosphere. As a result of the models' inability to produce the strengthened polar vortex, the observed surface warming and cooling were not well reproduced, either in spatial pattern or strength of the anomalies. In contrast to the findings of *Driscoll et al*. [2012], however, *Bittner et al*. [2016] showed that for the largest eruptions, the CMIP5 ensemble does produce a robust strengthening of the polar vortex, thereby further confounding the issue.

The perceived inability of climate models to produce this dynamical response in past studies has been attributed to weaknesses in the models, most notably the models' treatment of volcanic aerosol [*Stenchikov et al*., 2006; *Driscoll et al*., 2012]. Specifically, models commonly represent aerosol in four latitude bands, a highly simplified implementation [*Marshall et al*., 2009]. In addition, it has been posited that the models do not allow a sufficiently strong AO response to large-scale forcing [*Otterå*, 2008; *Driscoll et al*., 2012], though *Bittner et al*. [2016] show that this may not be the case. There is also debate as to whether the inclusion of ozone chemistry would improve model simulations of volcanic eruptions [*Stenchikov et al*., 2002; *Marshall et al*., 2009].

Both *Stenchikov et al*. [2006] and *Driscoll et al*. [2012] analyzed the mean anomalies of the first two posteruption winters of the nine largest tropical eruptions in the 1850–2005 period. However, *Robock and Mao* [1992] stated that the winter warming response should, in general, be expected only for the first winter following large tropical eruptions. Averaging the first two winters after each eruption may therefore have had a damping effect on any signal that was present in the results of these studies. In addition, we would not expect the models to exactly simulate the observations, so that evaluating a smaller eruption with a weaker observed winter warming response might have a similar damping effect. Therefore, in an effort to extract any winter warming signal that may be present in the models, we analyze only the first winter after the two largest eruptions in the 1850–2005 historical period. The models and experiments are described in section 2, results are presented in sections 3 and 4, and in section 5 we present our discussion and conclusions.

2. Models and Experiments

The model runs analyzed here are from the historical simulations (1850–2005) of CMIP5. Unlike some of the other external forcings (e.g., solar, greenhouse gases), which were standardized for the experiments, one of five volcanic forcing data sets—*Ammann et al*. [2003, 2007], *Sato et al*. [1993], *Stenchikov et al*. [1998], or *Andres and Kasgnoc* [1998]—was used by each modeling group. The volcanic forcing data set used by each model is given in Table S1 in the supporting information.

We chose to restrict analysis to those CMIP5 models that have at least two ensemble members for the historical experiment, and which had a realistic treatment of volcanic aerosols; that is, we excluded models which reduced the solar constant to achieve the radiative forcing associated with the eruption. Of the 22 models satisfying these requirements, we also discarded the two models (~10% of the set) with the lowest wintertime variability in 50 hPa geopotential height and zonal wind, as we would not expect these models to be able to produce an adequate response to the volcanic forcing. All available ensemble members were used for each model, with a total of 20 models and 122 ensemble members. Individual model means were calculated before the multimodel mean, so that all models were given equal weight. Table S1 lists the models and some details regarding each model.

In previous studies, the nine largest volcanic eruptions between 40°N and 40°S over 1883 to 2005 were analyzed [*Stenchikov et al*., 2006; *Driscoll et al*., 2012]; here we restricted our analysis to the two largest eruptions over that same latitude band and time frame, similarly to *Bittner et al*. [2016]. We have therefore analyzed the first winters and summers after the 1883 Krakatau and 1991 Pinatubo eruptions, with the exception of geopotential height, for which we have analyzed the 1982 El Chichón eruption in place of the Krakatau eruption. This distinction is made because of the choice of reanalysis data sets discussed below. See Table S2 for a brief description of the three volcanic eruptions considered.

In addition to the low number of observed volcanic eruptions considered here, high variability during NH winter and influence by other natural factors such as El Niño and the Quasi-Biennial Oscillation all contribute to a highly noisy volcanic signal with regard to the observations. However, the point of restricting the analysis to the two strongest volcanic eruptions, as was done by *Bittner et al*. [2016], is to examine whether including smaller eruptions in past studies has had the effect of masking the ability of CMIP5 models to reproduce this

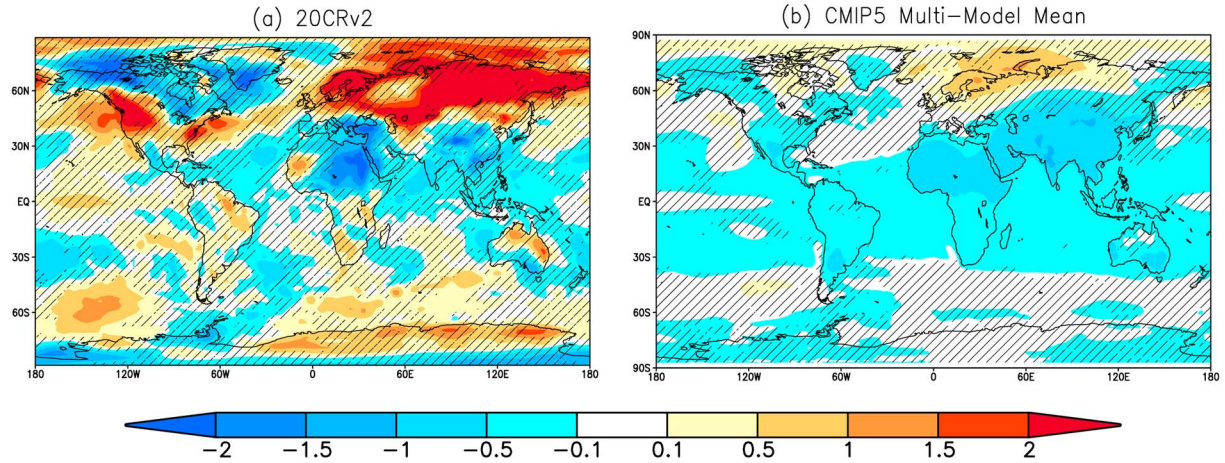

Figure 1. Surface temperature anomalies with respect to the 5 years preceding each eruption (K) for the first winter (DJF) after the 1883 Krakatau and 1991 Pinatubo eruptions for (a) 20CRv2 reanalysis and (b) CMIP5 model mean. Hatching displays areas below 90% significance (Figure 1a) and areas where fewer than 15 of 20 models agree on the sign of the anomaly (Figure 1b).

NH winter dynamical response to tropical volcanic eruptions. In addition, previous studies have examined the role of El Niño in the winter warming response as well as including observations of several more eruptions [*Robock and Mao*, 1992; *Stenchikov et al*., 2006; *Driscoll et al*., 2012]; while including more eruptions helps to average out some of the climate variability—resulting in an average response that is lower in amplitude—the spatial pattern of the response remains largely unchanged. Therefore, for the sake of consistency with the model analysis, we present the observations for the same two volcanic eruptions in each case.

For surface air temperature, mean sea level pressure, and precipitation, the reanalysis of the 20th Century version 2 (20CRv2) [*Compo et al*., 2011] is used for comparison with observations. In addition, and because of the high uncertainty in the 20CRv2 reconstructions of upper air fields [*Compo et al*., 2011], the ERA40 [*Uppala et al*., 2005] reanalysis fields are used to compare with lower stratosphere circulation changes during the winter season after the El Chichón and Pinatubo eruptions, as in *Driscoll et al*. [2012].

Previous studies have averaged the first two postvolcanic winters and have used different lengths of reference periods for each eruption [*Stenchikov et al*., 2006; *Driscoll et al*., 2012]. Here postvolcanic seasonal anomalies are calculated by subtracting the first NH winter (December-January-February (DJF)) and summer (June-July-August (JJA)) after each eruption from the same seasonal mean of the 5 years before the eruption. The statistical significance of anomalies for individual model means and observations is evaluated with a bootstrapping method. Specifically, for each model, and for the reanalysis data, we computed 5000 synthetic anomalies for each ensemble member. We calculated the ensemble mean of each of the 5000 synthetic data sets, and the 90% confidence interval for each model response is given by the 5% to 95% range of the 5000 synthetic means. Of course, statistical significance does not imply physical significance; i.e., high variability at high latitudes could cause a large anomaly to be considered insignificant, while low variability in the tropics could result in a small anomaly being significant there. For multimodel means, we quantify the level of model agreement in the sign of the response. Assessing the multimodel mean response in this manner may prevent one from discarding a small-magnitude response that is robust in that all of the simulations agree on the sign of the response, as well as highlighting large responses that may be dominated by only a few models [*Barnes et al*., 2016]. We define a significant response as one where at least 15 of the 20 models agree on the sign of the response. If the data were purely random, we would expect at least 15 of the 20 models to agree on the sign of the response 4.1% of the time, similar to a 95% confidence limit.

3. Winter Warming Response

3.1. Surface Temperature

Figure 1 shows the composite of DJF surface temperature anomalies after the eruptions. The reanalysis (Figure 1a) shows the well-documented significant surface warming signal over northern Europe and Asia,

where anomalies are almost everywhere above 2 K. Significant cooling is also observed over Northern Africa and the Middle East. The results here are based on only two postvolcanic winters and so natural climate variability will contribute to the observed response. However, previous observational studies including more eruptions have shown that this response is typical for large tropical eruptions [e.g., *Robock and Mao*, 1992]. Consistent with *Stenchikov et al*. [2006] and *Driscoll et al*. [2012], there is a warming signal in the Eastern Pacific. This, along with at least some of the warming over North America, can be attributed to the fact that both eruptions were at the same time as an El Niño, and the models should therefore, in general, not be expected to show the same pattern in these regions. The positive anomaly in the Arctic region appears unusually large, but the reliability of temperature at high latitudes is low, so the anomaly in this region might not be considered highly significant [*Compo et al*., 2011].

Though lower in magnitude and not reaching as far south, the multimodel mean of surface temperature does show significant warming over northern Eurasia, in agreement with observations (Figure 1b). This, in addition to the significant cooling over northern Africa and the Middle East, can be seen as a robust dynamical response to a large tropical volcanic eruption. Figure 1b shows the average response over all models, and Figure S1 in the supporting information shows the composites of surface temperature for the first postvolcanic winter for the individual models. As should be expected, there is plenty of variability between the models in their NH response. However, the observed warming in northern Eurasia is simulated by most of the models, though it is, in general, weaker and over smaller areas than in the observations. Some of the models, on the other hand (Australian Community Climate and Earth System Simulator version 1.3 (ACCESS1-3), Community Earth System Model 1-Fast Chemistry (CESM1-FASTCHEM), and the core version of the Norwegian Climate Center's Earth System Model (NorESM1-M)), show warming only in a small region, with a general cooling in the Asian-European area. Most of the models show significant cooling in the tropical latitudes, and all models but CESM1-Community Atmosphere Model version 5 (CAM5) show significant cooling in both Northern Africa and the Middle East, in agreement with the observations.

The analysis of surface temperature in the CMIP5 ensemble shows a better correspondence with observations during the first NH winter following large tropical eruptions than has been found previously by including smaller eruptions and averaging two winters [*Stenchikov et al*., 2006; *Driscoll et al*., 2012]. Figure S2a shows that there is good model agreement in the tropics (cooling) and over Northern Eurasia (warming). A significant improvement is seen—in comparison to the findings of *Stenchikov et al*. [2006] and *Driscoll et al*. [2012]—in the models' ability to produce surface warming over Eurasia and cooling over the Middle East. These improvements can be attributed to the difference on how the analysis was done, especially since *Driscoll et al*. [2012] used the same CMIP5 historical runs and many of the same participating models.

3.2. Mean Sea Level Pressure

The reanalysis shows significant negative anomalies in the mean sea level pressure over the Arctic region and significant positive anomalies over the North Atlantic (Figure 2a). This pattern suggests that the observed surface temperature anomalies are related to changes in the winter circulation caused by the volcanic eruptions. These sea level pressure anomalies are consistent with a positive phase of the NAO and are in agreement with previous studies [*Stenchikov et al*., 2006; *Driscoll et al*., 2012].

The multimodel composite of mean sea level pressure (Figure 2b) shows a similar pattern to the observations, with somewhat significant negative anomalies over the Arctic and more positive anomalies equatorward. On the other hand, the anomalies are of lesser magnitude, and the strong positive anomaly seen over the North Atlantic is not captured in the model mean. Instead, the maximum positive anomaly in the multimodel mean is shifted over Europe. While some models are able to produce the observed positive NAO-like pattern (Second Generation Canadian Earth System Model (CanESM2), Geophysical Fluid Dynamics Laboratory Climate Model version 3 (GFDL-CM3), Hadley Climate Model version 3, E2-H version of the Goddard Institute for Space Studies (GISS-E2-H), and NorESM1-M), Figure S2b shows much disagreement in the sign of the anomalies and Figure S3 shows large differences in sea level pressure patterns between models. Indeed, many of the models do produce a dipole, though several (e.g., Beijing Climate Center-Climate System Model version 1.1 (bcc-csm1-1), Max-Planck-Institut-Earth System Model running on mixed resolution grid (MPI-ESM-MR), and Centre National de Recherches

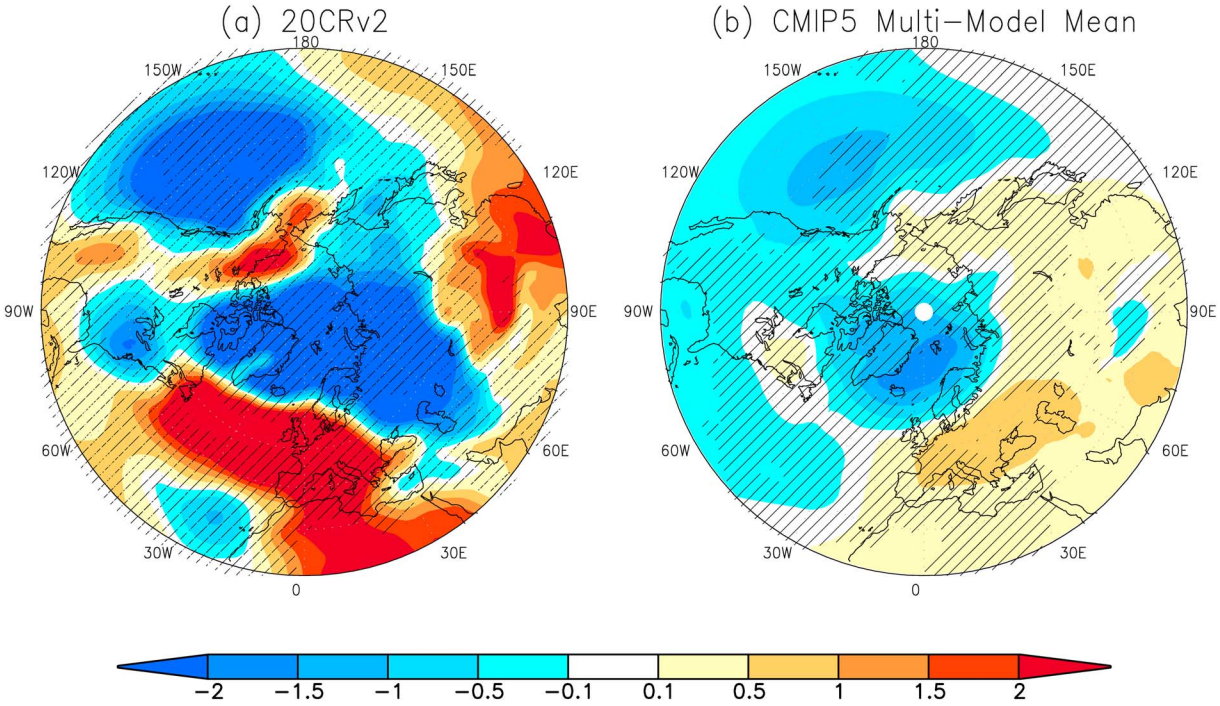

Figure 2. Sea level pressure anomalies with respect to the 5 years preceding each eruption (hPa) for the first winter (DJF) after the 1883 Krakatau and 1991 Pinatubo eruptions for (a) 20CRv2 reanalysis and (b) CMIP5 model mean. Hatching displays areas below 90% significance (Figure 1a) and areas where fewer than 15 of 20 models agree on the sign of the anomaly (Figure 1b).

Météorologiques climate model version 5) have the maximum positive anomaly shifted over Europe, as shown in the multimodel mean. Still, others show anomaly patterns of opposite sign to the observations (Community Climate System Model version 4 and CESM1-FASTCHEM).

3.3. Geopotential Height

Geopotential height anomalies in the stratosphere help define circulation changes during winters following large volcanic eruptions. Due to the high uncertainty in the 20CRv2 reconstructions of upper air fields for the preradiosonde era, we analyze here the El Chichón and Pinatubo eruptions by using the ERA40 data set. In observations the anomaly pattern in the stratosphere shows a cold and deep polar night vortex, as observed in the 50 hPa geopotential height anomalies (Figure 3a) showing a large statistically significant decrease in geopotential height over the pole and over Northern Europe, with positive anomalies observed at lower latitudes. This has previously been attributed to the direct heating of the lower tropical stratosphere by the volcanic aerosols [*Stenchikov et al.*, 1998; *Ramachandran et al.*, 2000]. The observed negative anomaly in 50 hPa geopotential height at high latitudes points to a colder lower stratosphere near the pole, which suggests a stronger and persistent polar vortex [*Driscoll et al.*, 2012]. Previous studies also suggest that this might be a characteristic of the early stage of the postvolcanic winter season [*Graf et al.*, 2007; *Mitchell et al.*, 2011].

The multimodel mean 50 hPa geopotential height anomalies (Figure 3b) show a similar strengthening of the polar vortex, with a significant positive anomaly moving equatorward, though the magnitude of these anomalies is in some areas different from those in the observations. Most of the models show the same general pattern observed in the stratosphere (see Figure S4) as in the reanalysis, though the magnitude of the responses varies considerably. In particular, the maximum observed increase in geopotential height is over North America (Figure 3a), while the maximum positive anomalies are shifted toward the Pacific Ocean in many of the models (Figures 3b and S4). In addition, while most models show the positive change in geopotential height in the tropics and midlatitudes, some models fail to reproduce the strong negative anomalies in the lower polar stratosphere. ACCESS1-3, CESM1-CAM5, CESM1-FASTCHEM, bcc-csm1-1, and MPI-ESM-MR show good spatial agreement with the reanalysis, with anomalies in ACCESS1-3 and the

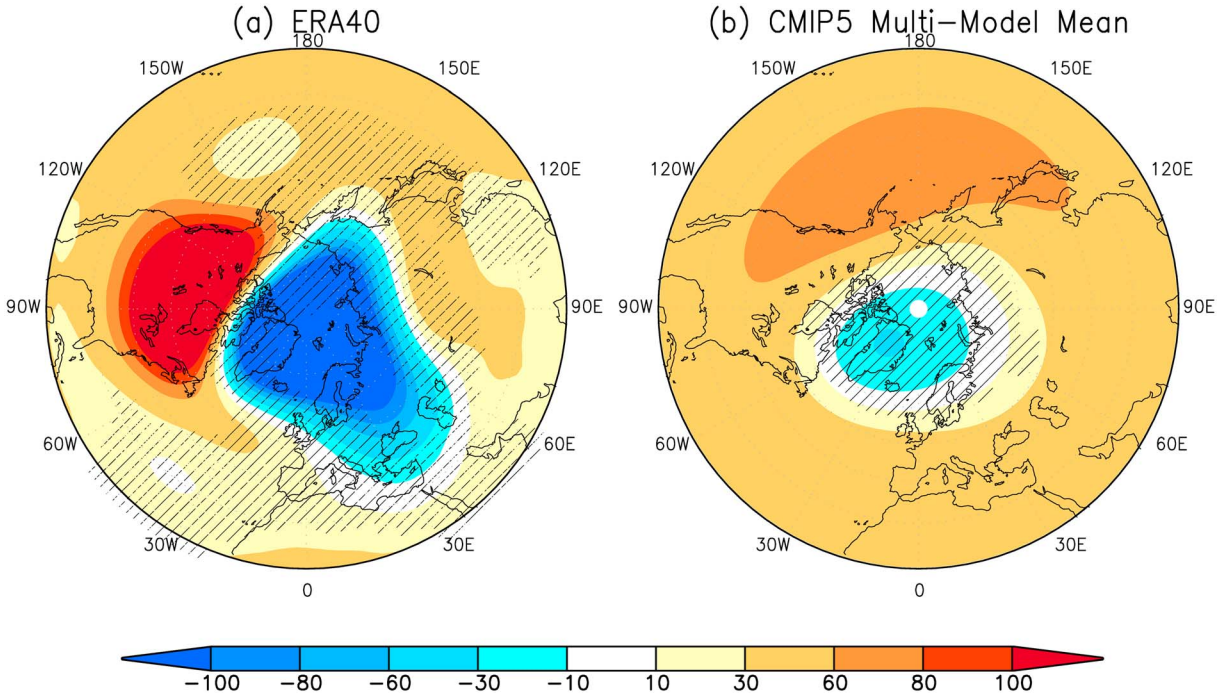

Figure 3. Geopotential height anomalies with respect to the 5 years preceding each eruption at 50 hPa (m) for the first winter (DJF) after the 1982 El Chichón and 1991 Pinatubo eruptions for (a) ERA40 reanalysis and (b) CMIP5 model mean. Hatching displays areas below 90% significance (Figure 1a) and areas where fewer than 15 of 20 models agree on the sign of the anomaly (Figure 1b).

CESM1 models reaching above 100 m in the tropics and midlatitudes and below −100 m at the pole. NorESM1-M also shows similar patterns, though the vortex is centered over Northern Europe and North America/Greenland, respectively. GFDL-CM3 shows almost no change in circulation with regard to the 50 hPa geopotential height, and both Institut Pierre-Simon Laplace (IPSL) models, which were excluded because of not using aerosol forcing, show the opposite pattern, with positive anomalies near the pole and negative anomalies equatorward. However, the GFDL-CM3 and IPSL-Climate Model 5A-Medium Resolution did produce strong winter warming patterns (Figure S1), showing that it is possible to get that pattern without stratospheric forcing, as was found for an older GFDL model [*Stenchikov et al.*, 2002]. The relative strength of these different mechanisms will be studied in Tier 1 simulations of the upcoming Volcanic Model Intercomparison Project (VolMIP) *Zanchettin et al.*, 2016] but is beyond the scope of the present work.

4. Summer Monsoon Reduction

Circulation changes and indirect effects of sulfate aerosols due to large volcanic eruptions are thought to reduce summer precipitation in Northern Africa and Asia [*Rotstayn and Lohmann*, 2002; *Thordarson and Self*, 2003; *Oman et al.*, 2006; *Iles and Hegerl*, 2014]. *Robock and Liu* [1994] pointed out that the Sahel region had its lowest rainfall over 1940–1990 in the summers directly following the 1982 El Chichón eruption, suggesting that large tropical eruptions may tend to strengthen droughts in the region. Observations of summer precipitation after the 1883 Krakatau and 1991 Pinatubo eruptions are consistent with these findings, showing a significant reduction in summer precipitation over the Sahel region and over the Maritime Continent, with anomalies below −2 mm/d in some areas (Figure 4a). On the other hand, observations show a significant increase in precipitation over parts of India, though historical accounts and previous studies show that volcanic eruptions have been associated with droughts in the region [*Mooley and Pant*, 1981; *Oman et al.*, 2006]. The multimodel mean (Figure 4b) shows drying in all three regions mentioned, agreeing with previous studies and not the observations with regard to changes in rainfall over India. Negative anomalies are significant over India and in some areas over the Maritime Continent and the Sahel.

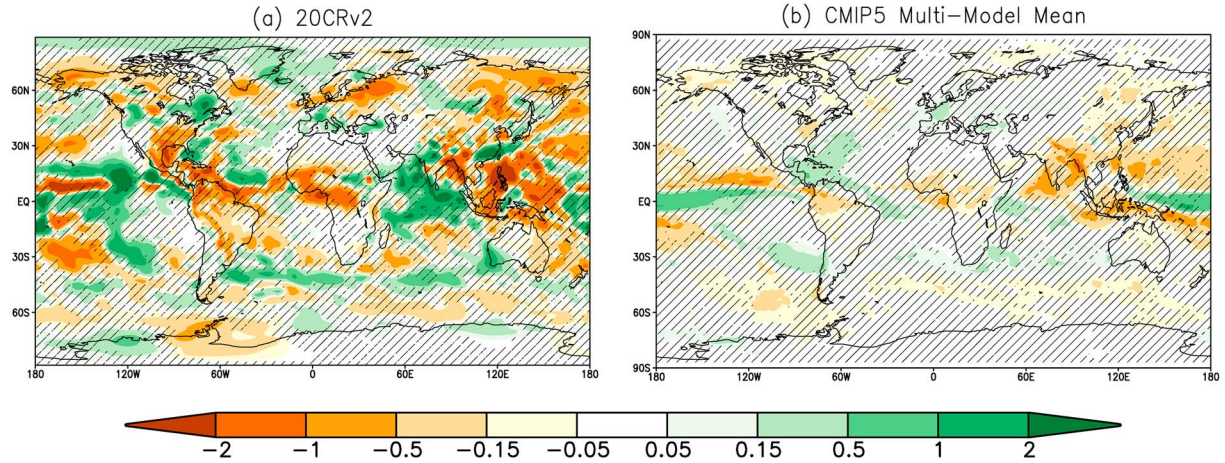

Figure 4. Precipitation anomalies with respect to the 5 years preceding each eruption (mm/d) for the first summer (JJA) after the 1883 Krakatau and 1991 Pinatubo eruptions for (a) 20CRv2 reanalysis and (b) CMIP5 model mean. Hatching displays areas below 90% significance (Figure 1a) and areas where fewer than 15 of 20 models agree on the sign of the anomaly (Figure 1b).

Over the period of 1851–2012, the mean tropical (30°S–30°N) JJA precipitation in the 20CRv2 reanalysis is 3.6 mm/d with a standard deviation of 2.0 mm/d, about 56% of the mean. Due to this high variance in precipitation, high variability between models is shown in Figures S2d and S5. Most of the models show significant drying over the Sahel region, though GISS-E2-H, NorESM1-M, CESM1-CAM5, and CESM1-FASTCHEM show more positive anomalies than negative there. MPI-ESM-MR and GISS-E2-H are the only models that do not show significant drying over India; MPI-ESM-MR has India wetter during the postvolcanic summers, while GISS-E2-H shows no change in precipitation.

5. Discussion and Conclusions

Previous studies have concluded that current global climate models do a poor job of reproducing circulation changes and the associated NH warming response during winters after large tropical volcanic eruptions [*Stenchikov et al.*, 2006; *Driscoll et al.*, 2012; *Charlton-Perez et al.*, 2013]. These studies, however, calculated anomalies by calculating the average of the first two postvolcanic winters while—on the average—one would expect winter warming to last only the first winter after the eruption for large tropical eruptions [*Robock and Mao*, 1992]. More recently, however, *Bittner et al.* [2016] obtained more positive results by using different methods of analysis than those shared by the previous studies. By considering only the first winter after the eruptions, and by considering only the two largest eruptions, we have shown that climate models in the CMIP5 ensemble are capable of producing these circulation changes and temperature responses for large enough eruptions, in agreement with *Bittner et al.* [2016], who found that the mean of 15 CMIP5 models did simulate a positive AO in the first NH winter after the 1883 Krakatau and 1991 Pinatubo eruptions. We also did our analysis with all nine larger tropical eruptions over the historical period and found similar, but damped responses (see Figure S6). Consistent with the results of *Bittner et al.* [2016], the volcanic signal is somewhat lost when smaller eruptions are considered.

CanESM2 simulates the climate that is most comparable to the observed winter warming response, doing a fairly good job of reproducing changes in surface temperature, sea level pressure, and circulation. bcc-csm1-1 and CESM1-FASTCHEM both show a realistic warming pattern and a strong polar vortex through 50 hPa geopotential height changes but fail to produce the positive phase of the NAO as illustrated by changes in sea level pressure. GFDL-CM3 is in good agreement with observations in both temperature and sea level pressure but shows very little change in 50 hPa geopotential height.

Not all of the CMIP5 models produced a good winter warming or summer monsoon response following the 1883 Krakatau and 1991 Pinatubo eruptions, but 16 of them did. They are indicated in Table S1, and the patterns they produced, which are stronger than those shown here, are shown in Figure S7. As has been pointed out in previous studies [*Driscoll et al.*, 2012; *Maher et al.*, 2015], in addition to different forcing data sets, some

of the models differ in their implementation of volcanic forcing. However, these differences do not have an impact on the overall results. Indeed, we examined the differences in forcing, model resolution, model top, and their ability to simulate AO and could not find any criteria that would allow us to determine a priori which models did a good simulation. Of course, it may have been by chance because of the small number of ensemble members.

While we would not expect climate models on average to exactly simulate the observed response, which includes random variability, these results give us confidence that the CMIP5 models, in general, can simulate responses to large volcanic eruptions similar to those observed. Using the CMIP6 models, with improvements such as higher resolution and a more realistic treatment of aerosols, VolMIP [*Zanchettin et al*., 2016] will look to build upon these results.

Acknowledgments
This work is supported by National Science Foundation grant AGS-1430051. We thank the Centre for Environmental Data Analysis (http://ceda.ac.uk) for making the CMIP5 output available and the reviewers for valuable comments, which improved the manuscript.

References

Ammann, C. M., F. Joos, D. S. Schimel, B. L. Otto-Bliesner, and R. A. Tomas (2007), Solar influence on climate during the past millennium: Results from transient simulations with the NCAR Climate System Model, *Proc. Natl. Acad. Sci. U.S.A.*, *104*, 3713–3718.

Ammann, C. M., G. A. Meehl, W. M. Washington, and C. S. Zender (2003), A monthly and latitudinally varying volcanic forcing dataset in simulations of 20th century climate, *Geophys. Res. Lett.*, *30*(12), 1657, doi:10.1029/2003GL016875.

Andres, R. J., and A. D. Kasgnoc (1998), A time averaged inventory of subaerial volcanic sulphur emissions, *J. Geophys. Res.*, *103*, 25,251–25,261, doi:10.1029/98JD02091.

Barnes, E., S. Solomon, and L. Polvani (2016), Robust wind and precipitation responses to the Mount Pinatubo eruption, as simulated in the CMIP5 models, *J. Clim.*, *29*, 4763–4778, doi:10.1175/JCLI-D-15-0658.1.

Bittner, M., H. Schmidt, C. Timmreck, and F. Sienz (2016), Using a large ensemble of simulations to assess the Northern Hemisphere stratospheric dynamical response to tropical volcanic eruptions and its uncertainty, *Geophys. Res. Lett.*, *43*, 9324–9332, doi:10.1002/2016GL070587.

Charlton-Perez, A. J., et al. (2013), On the lack of stratospheric dynamical variability in low-top versions of the CMIP5 models, *J. Geophys. Res. Atmos.*, *118*, 2494–2505, doi:10.1002/jgrd.50125.

Christiansen, B. (2008), Volcanic eruptions, large-scale modes in the Northern Hemisphere, and the El Niño–Southern Oscillation, *J. Clim.*, *21*, 910–922.

Compo, G. P., et al. (2011), The twentieth century reanalysis project, *Q. J. R. Meteorol. Soc.*, *137*(654), 1–28, doi:10.1002/qj.776.

Driscoll, S., A. Bozzo, L. J. Gray, A. Robock, and G. Stenchikov (2012), Coupled Model Intercomparison Project 5 (CMIP5) simulations of climate following volcanic eruptions, *J. Geophys. Res.*, *117*, D17105, doi:10.1029/2012JD017607.

Graf, H.-F., Q. Li, and M. A. Giorgetta (2007), Volcanic effects on climate: Revisiting the mechanisms, *Atmos. Chem. Phys.*, *7*(17), 4503–4511, doi:10.5194/acp-7-4503-2007.

Hurrell, J. W. (1995), Decadal trends in the North Atlantic Oscillation: Regional temperatures and precipitation, *Science*, *269*, 676–679.

Iles, C. E., and G. C. Hegerl (2014), The global precipitation response to volcanic eruptions in the CMIP5 models, *Environ. Res. Lett.*, *9*, doi:10.1088/1748-9326/9/10/104012.

Kodera, K., M. Chiba, H. Koide, A. Kitoh, and Y. Nikaidou (1996), Interannual variability of the winter stratosphere and troposphere in the Northern Hemisphere, *J. Meteorol. Soc. Jpn.*, *74*, 365–382.

Maher, N., S. McGregor, M. H. England, and A. Sen Gupta (2015), Effects of volcanism on tropical variability, *Geophys. Res. Lett.*, *42*, 6024–6033, doi:10.1002/2015GL064751.

Marshall, A. G., A. A. Scaife, and S. Ineson (2009), Enhanced seasonal prediction of European winter warming following volcanic eruptions, *J. Clim.*, *22*(23), 6168–6180, doi:10.1175/2009JCLI3145.1.

Mitchell, D. M., L. J. Gray, and A. J. Charlton-Perez (2011), The structure and evolution of the stratospheric vortex in response to natural forcings, *J. Geophys. Res.*, *116*, D15110, doi:10.1029/2011JD015788.

Mooley, D. A., and G. B. Pant (1981), Droughts in India over the last 200 years, their socio-economic impacts and remedial measures for them, in *Climate and History: Studies in Past Climates and Their Impact on Man*, edited by T. M. L. Wigley, M. J. Ingram, and G. Farmer, pp. 465–478, Cambridge Univ. Press, New York.

Oman, L., A. Robock, G. L. Stenchikov, and T. Thordarson (2006), High-latitude eruptions cast shadow over the African monsoon and the flow of the Nile, *Geophys. Res. Lett.*, *33*, L18711, doi:10.1029/2006GL027665.

Otterå, O. H. (2008), Simulating the effects of the 1991 Mount Pinatubo volcanic eruption using the ARPEGE atmosphere general circulation model, *Adv. Atmos. Sci.*, *25*, 213–226, doi:10.1007/s00376-008-0213-3.

Perlwitz, J., and H.-F. Graf (1995), The statistical connection between tropospheric and stratospheric circulation of the Northern Hemisphere in winter, *J. Clim.*, *8*, 2281–2295.

Ramachandran, S., V. Ramaswamy, G. L. Stenchikov, and A. Robock (2000), Radiative impact of the Mount Pinatubo volcanic eruption: Lower stratospheric response, *J. Geophys. Res.*, *105*, 24,409–24,429, doi:10.1029/2000JD900355.

Robock, A. (2000), Volcanic eruptions and climate, *Rev. Geophys.*, *38*, 191–219, doi:10.1029/1998RG000054.

Robock, A., and Y. Liu (1994), The volcanic signal in Goddard Institute for Space Studies three-dimensional model simulations, *J. Clim.*, *7*, 44–55.

Robock, A., and J. Mao (1992), Winter warming from large volcanic eruptions, *Geophys. Res. Lett.*, *19*, 2405–2408, doi:10.1029/92GL02627.

Robock, A., and J. Mao (1995), The volcanic signal in surface temperature observations, *J. Clim.*, *8*, 1086–1103.

Rotstayn, L. D., and U. Lohmann (2002), Tropical rainfall trends and the indirect aerosol effect, *J. Clim.*, *15*, 2103–2116.

Sato, M., J. E. Hansen, M. P. McCormick, and J. B. Pollack (1993), Stratospheric aerosol optical depths, 1850–1990, *J. Geophys. Res.*, *98*, 22,987–22,994, doi:10.1029/93JD02553.

Stenchikov, G., K. Hamilton, R. J. Stouffer, A. Robock, V. Ramaswamy, B. Santer, and H.-F. Graf (2006), Arctic Oscillation response to volcanic eruptions in the IPCC AR4 climate models, *J. Geophys. Res.*, *111*, D07107, doi:10.1029/2005JD006286.

Stenchikov, G. L., I. Kirchner, A. Robock, H.-F. Graf, J. C. Antuña, R. G. Grainger, A. Lambert, and L. Thomason (1998), Radiative forcing from the 1991 Mount Pinatubo volcanic eruption, *J. Geophys. Res.*, *103*, 13,837–13,857, doi:10.1029/98JD00693.

Stenchikov, G., A. Robock, V. Ramaswamy, M. D. Schwarzkopf, K. Hamilton, and S. Ramachandran (2002), Arctic Oscillation response to the 1991 Mount Pinatubo eruption: Effects of volcanic aerosols and ozone depletion, *J. Geophys. Res.*, *107*(D24), 4803, doi:10.1029/2002JD002090.

Taylor, K. E., R. J. Stouffer, and G. A. Meehl (2012), An overview of CMIP5 and the experiment design, *Bull. Am. Meteorol. Soc.*, *93*, 485–498, doi:10.1175/BAMS-D-11-00094.1.

Thompson, D. W. J., and J. M. Wallace (1998), The Arctic Oscillation signature in the wintertime geopotential height and temperature fields, *Geophys. Res. Lett.*, *25*, 1297–1300, doi:10.1029/98GL00950.

Thordarson, T., and S. Self (2003), Atmospheric and environmental effects of the 1783–1784 Laki eruption: A review and reassessment, *J. Geophys. Res.*, *108*(D1), 4011, doi:10.1029/2001JD002042.

Uppala, S. M., et al. (2005), The ERA-40 re-analysis, *Q. J. R. Meteorol. Soc.*, *131*(612), 2961–3012, doi:10.1256/qj.04.176.

Zanchettin, D., et al. (2016), The Model Intercomparison Project on the climatic response to Volcanic forcing (VolMIP): Experimental design and forcing input data, *Geosci. Model Dev.*, *9*, 2701–2719, doi:10.5194/gmd-9-2701-2016.